Geothermal reservoir potential of volcaniclastic settings: The Valley of Mexico, Central Mexico

Abstract

The geothermal potential of the Valley of Mexico has not been addressed in the past, although volcaniclastic settings in other parts of the world contain promising target reservoir formations. An outcrop analogue study of the thermophysical rock properties of the Neogene rocks within the Valley of Mexico was conducted to assess the geothermal potential of this area. Permeability and thermal conductivity are key parameters in geothermal reservoir characterization and the values gained from outcrop samples serve as a sufficient database for further assessment. The mainly low permeable lithofacies types may be operated as stimulated systems, depending on the fracture porosity in the deeper subsurface. In some areas also auto-convective thermal water circulation might be expected and direct heat use without artificial stimulation becomes reasonable. Thermophysical properties of tuffs and siliciclastic rocks qualify them as target horizons for future utilization of deep geothermal reservoirs.

Keywords: Volcaniclastics; thermophysical rock properties; renewable energy sources; Valley of Mexico; geothermal energy; energy storage

1. Introduction

In recent years the efficient use of energy resources and energy storage has gained great importance. For the future, increasing global energy demand strongly relies on renewable energy development (e.g. geothermal, wind, and solar energy) that may reduce the dependence on fossil fuels and its related negative effects for the environment. Right now, Mexico is still mainly based on fossil-fueled (hydrocarbons and coal, 68%) power plants, and more than one fifth (22%) on hydroelectric plants. Geothermal electric capacity represents 2%

and wind only 0.1%. The rest (1.9%) is represented by nuclear power plants. The solar potential for electricity is largely untapped, leaving room for great improvements in the future [1].

Mexico has among the best potential for solar power in the world [2], and according to the World Energy Council [3] report “the scope for solar electricity generation is unlimited from a technological point of view”. More than 70% of the country's surface receives an insolation in excess of 4.7 kWh/m^2/day (1,700 kWh/m^2/yr), which corresponds to 50 times national electricity generation. Electricity produced by photovoltaics in Mexico in 2008 is reported as 9.277 GWh [4]. At the Solar Power Mexico 2012 conference in Mexico City, it was said that photovoltaics electricity and solar thermal will comprise up to 5% of Mexico's energy by 2030 and up to 10% by 2050. Most of the already existing solar power stations can be found in Sonora and the Baja California or are supposed to be commissioned, soon. In Sonora, the average sunlight hours per day are 6.4 with an average of 7 kWh/m^2/day (2556.7 kWh/m^2/yr). But even in Mexico City, with 7.6 average sunlight hours per day, there is still an average of 5 kWh/m^2/day (1826.2 kWh/m^2/yr), also making the Valley of Mexico, that this paper will focus on, a possible location for the construction of solar power plants in order to provide the 21.2 million people of the metropolitan area of Mexico City with electricity.

The total generation capacity for Mexican wind energy was calculated for 2013 to 1,488 MW, finally making wind energy a competitive option within the Mexican electricity market [5, 6]. So far, Mexican wind farms have been limited to smaller projects in Oaxaca (La Venta and La Ventosa wind farms). Nevertheless, the Comisión Reguladora de Energía (CRE) has issued permits for wind plants in Baja California, Tamaulipas, Nuevo León, San Luis Potosí, Veracruz, and Chiapas, bringing the total number of wind power generation permits issued to 30 across the country within the next few years [7].

One of the biggest problems holding back renewable energy is that energy sources such as wind and the sun, are not constant, and therefore do not allow a steady output. The best way

of overcoming this problem is by developing energy storage systems that can store excess energy produced during times of high output, and release it again when it is needed during times of low output. Energy from both sources, wind and sun, can be stored in porous rocks deep underground for later use. Wind energy – which is often produced at night when winds are strong and energy demand is low – can be stored by a method called compressed air energy storage (CAES) [8, 9]. The basic idea of CAES is to capture and store compressed air in suitable geologic structures underground when off-peak power is available or additional load is needed on the grid for balancing. The stored high-pressure air is returned to the surface and used to produce power when additional generation is needed, such as during peak demand periods [10].

Underground thermal energy storage (UTES) [11, 12, 13, 14] is a system that uses inter-seasonal heat storage, storing excess heat (e.g. from solar collectors) for use in winter heating, and the cooling potential from winter for cooling in summer [15]. This could contribute significantly to meeting society's need for heating and cooling. UTES may be implemented in rocks or soil via a series of vertical borehole heat exchangers or in deep aquifers [16].

Finally, the development of so-called hybrid systems combining solar/wind, geothermal and biomass energy is seen as very promising in countries like Mexico.

According to the Global Energy Network Institute [17] Mexico has an estimated geothermal electricity potential of at least 8,000 MWe, second in the world only to Indonesia. In reality, Mexico is not that far, yet, in harvesting this geothermal potential to the maximum. Nevertheless, with 980 MW [18] (887 MW according to the World Energy Council [19]), the country is ranked fourth in terms of global installed geothermal capacity (after the U.S. (3,098 MW), the Phillipines (1,904 MW), and Indonesia (1,197 MW); values according to Bertani [20]).

The currently four operating geothermal fields in Mexico are Cerro Prieto (a geothermally active area intersecting the southern end of the Imperial Fault and the northern end of the

Cerro Prieto Fault in the Baja California), Las Tres Vírgenes (related to a complex of volcanoes located in the Mulegé Municipality in the state of Baja California Sur), Los Azufres, and Los Humeros. The project Cerritos Colorados, formerly known as La Primavera, has been scheduled for 2014 [21]. The three latter geothermal fields are all part of the Transmexican Volcanic Belt and are associated to large calderas [22], which could, in the future, be the source for a lot more energy for Mexico and also the U.S., considering that in 2012 already 1,285,959 MWh had been exported to the northern neighbor [23].

In Mexico, geothermal energy is almost entirely used to produce electricity. The direct use of Mexican geothermal energy is still under development and currently remains restricted to bathing and swimming facilities. The use of geothermal heat pumps is minimal, and underdeveloped with no information available [24]. Furthermore, to date, no useful information is available on the geothermal gradients of the Mexican deep sedimentary basins or graben settings, such as the Valley of Mexico [25, 26, 27], and its possible potential for a direct use of geothermal energy.

The Valley of Mexico, located in the Transmexican Volcanic Belt, contains most of the Mexico City Metropolitan Area, as well as parts of the State of Mexico, Hidalgo, Tlaxcala and Puebla, and can be subdivided into four sub-basins [28]. The surrounding mountain ranges of the Sierra de Las Cruces, Sierra Nevada, and Sierra Chichinautzin are (in decreasing order) the main recharge areas for the enclosed basin [29].

Below a 30 to >200 m thick cover of Quaternary to recent volcanic and lake deposits [25, 30, 31] that outcrop extensively on the plain, Neogene volcanic rocks (intercalated with siliciclastic and volcaniclastic rocks) attain a thickness of up to 4000 m [25, 26, 32] on top of the basement. These units are extensively fractured and crossed by fault (graben) systems that resulted from tensional regional forces [33]. They partially cover an excess thickness of 1000 m of limestone strata of Cretaceous age.

A reasonable amount of data is available only on the hydraulic properties of the Pliocene–Quaternary and Quaternary–Recent deposits. The properties of the deeper aquifer units, however, are not known [25]. However, several hundreds of liters of water per second that are continuously extracted from the Mid Tertiary volcanics for the dewatering of a mine [34] in a mine district in the northern part of the Basin of Mexico, i.e. in Pachuca (Hidalgo State), are evidence for an effective reservoir and aquifer [35]. Furthermore, Carrillo-Rivera et al. [36] interpreted the hydraulic conductivity of the deeper aquifer from shallow boreholes (~300 m depth) in the northern part of the catchment.

Due to the lack of detailed well logs and physical data of this area, a pilot study was initiated on the Lower Miocene Tepoztlán Formation, which is supposed to be linked to the processes forming the Valley of Mexico [37]. Furthermore, the Tepoztlán Formation shows excellent exposures of its volcanic rocks, enabling an outcrop analog study of the thermophysical rock properties of the Neogene rocks within the Valley of Mexico. Recently, the Tepoztlán Formation rocks have been studied in detail, with a fairly complete geologic history already established [35, 38, 39, 40, 41].

The aim of this study is to provide thermophysical rock properties of the different lithofacies types to be added as important attributes into 3D reservoir models, identifying target formations for geothermal reservoir utilization.

2. Geological setting

The Valley of Mexico refers to the lower part of the Basin of Mexico (Fig. 1). The Basin of Mexico is one of the largest of a series of closed catchments located in the Transmexican Volcanic Belt [42, 43]. The eastern boundary of the catchment is characterized by the Sierra Nevada and its volcanoes such as the 5,400 m asl Popocatépetl and the 5,230 m asl Iztaccíhuatl. It is a closed basin located on a graben structure, which developed during the Oligocene, characterized by a thick sequence of volcanic and lacustrine deposits [25]. In those

times the basin drained to the south. The runoff outlet was closed during the Pleistocene as the result of a series of volcanic activities [44] that formed the monogenetic volcanic fields of the Sierra de Chichinautzin to the south of the basin [25], the Tezontepec Sierra to the northeast, and Teotihuacan to the north of the catchment [27]. The floor of the Valley of Mexico has an elevation of ca. 2236 m asl and the lowest part is still occupied by what remains of Lake Texcoco. The drainage divides in the mountains that surround the Valley are frequently more than 3000 m asl, and the lowest pass across the divide is about 2260 m asl [45]. Groundwater recharge occurs in the volcanic rocks of the mountains that surround the valley to form the Basin of Mexico [45].

The groundwater temperature towards the west of Mexico City is 19±1°C and increases to a fairly uniform 23±1°C near the centre of the basin [25]. The latter temperature is spatially related to the two thermal water spring sites that are reported from the Basin of Mexico, i.e. the thermal site of Peñon de los Baños (44°C), adjacent to the international airport [25, 46], and Peñon del Marquez [47]. After an increase in groundwater extraction in the 1950's, the thermal water is tapped solely by boreholes with a distinct discharge temperature of 45°C [26]. Direct temperature logging in a nearby borehole showed a temperature of 87°C at a depth of 1800 m [48, 49]. According to Huizar-Alvarez et al. [26], the observed temperature of the sampled water is in agreement with the natural geothermal gradient of ca. 3.16°C/100 m as the closest active volcanic area is located ca. 40 km to the southeast. Edmunds et al. [25] infer either a variable geothermal gradient across the basin or, that the water is being drawn up by abstraction, from greater depth beneath the city. By means of a silica geothermometer, Fournier [50] calculated an equilibrium temperature of 163°C in a depth of at least 2500 m (at an assumed geothermal gradient of 3.16°C/100 m).

Seismic studies and deep wells (drilled by PEMEX, Petróleos Mexicanos) in the Basin of Mexico reaching 4000 m, give evidence that the volcaniclastic succession in the lower unit of the basin is correlative with the Miocene Tepoztlán Formation [37, 51] (Fig. 2). The time of

the deposition of the Tepoztlán Formation is likely concurrent with the main phase of formation of the basin [35].

The Tepoztlán Formation crops out in an area of approximately 180 km^2 and has an overall maximum thickness of 800 m. The volume of the deposited material, still remaining after erosion, was calculated to 130 km^3 with the help of GIS. The formation is widespread around the villages of Malinalco and Chalma in Mexico State and Tepoztlán and Tlayacapan in Morelos State; sparse outcrops are located east of Tlayacapan and southeast of the Nevado de Toluca [52, 53].

A variety of Eocene-Oligocene (Balsas Group) and older rocks, mostly Cretaceous limestones, underlie the formation. It is covered by lava flows of Pliocene to Holocene age. Close to Malinalco, the Tepoztlán Formation crops out between the San Nicolás Basaltic Andesite and the overlying Basal Mafic Sequence [54]. In Tepoztlán and the eastern vicinities it unconformably overlies the Balsas Group and is covered by the Chichinautzin Formation.

The Tepoztlán Formation is composed of calc-alkaline volcanic and sedimentary rocks. The volcanic rocks have predominantly andesitic to dacitic compositions; however, rhyolites are also present [38]. The entire succession comprises pyroclastic deposits (fall, surge and flow deposits), deposits from lahars (debris-flow and hyperconcentrated-flow deposits) and coarse to fine fluvial and lacustrine deposits (conglomerates, sandstones and mudstones). Only few lava flows and dikes are present [39].

Clasts within the sediments are commonly coarsely porphyritic (20%-30% crystals) with plagioclase (anorthite), sanidine, augite, hornblende (magnesioriebeckite) and minor muscovite phenocrysts in a microcrystalline groundmass. The red, oxidized groundmass of many clasts indicates subaerial eruptions.

Bedding within the Tepoztlán Formation is generally flat-lying or gently dipping with up to 10° to N/NNE. The succession is disrupted by normal faults and dikes. Displacements at faults are frequently about half a meter and rarely exceed a few meters.

Magnetostratigraphy combined with K/Ar and Ar/Ar geochronology revealed an age of Early Miocene (22.75-18.78 Ma) [38].

3. Materials and methods

This study is based on an integrated analysis of petrographical and petrophysical data from the Tepoztlán Formation. 125 core samples from tuff, lava, tuffaceous breccia, conglomerates and sandstone with diameters of 5 cm were obtained by using a gasoline-driven drilling machine with diamond-studded drill heads. Core descriptions were prepared, detailing lithology, degree of welding, and alteration, as well as the nature and intensity of pore space and fractures. Petrographic analyses were conducted on thin sections prepared from selected core-plug samples.

Permeability measurements were carried out by usage of conditioned compressed air, using a gas pressure mini-permeameter, developed at the Institute of Applied Geosciences, TU Darmstadt, Germany. All samples were dried overnight in a conventional oven at 38° - 49°C before the measurements.

For the determination of the thermal conductivity the Optical Scanning Method was applied [56] on a Thermal Conductivity Scanner developed by “Lippmann and Rauen GbR”. In this method the surface temperature of the sample is measured contactless by infrared temperature sensors before and after heating with a contactless heat source. The sensors and the heat source move with constant speed and constant distance to each other along the sample and reference samples with known thermal conductivities. The determination of thermal conductivity is based on the comparison of the difference of the temperature of reference samples with known thermal conductivities and sample material with unknown thermal conductivity. As reference sample a material with a thermal conductivity in the range of the estimated thermal conductivity of the sample is used.

4. Results

4.1. Petrography

The studied samples consist of lavas and tuffs of dacitic to andesitic composition as previously identified by Lenhardt et al. [38]. Furthermore, samples from tuffaceous breccias, derived from mass-flow deposits (lahar deposits), and conglomerates and sandstones (siliciclastic rocks) [35, 39] were analyzed.

4.1.1. Lava samples

The lava has a porphyritic to glomeroporphyritic texture with phenocryst contents up to 60 vol.%. The mineral phases consist of plagioclase, subordinate K-feldspar, clinopyroxene and amphibole. Accessory phases consist of mica, abundant titanomagnetite and other accessories. The tuff samples consist of plagioclase, K-feldspar, subordinate pyroxene (augite) and rare quartz crystals in an ash-rich matrix. Subangular cognate lithic clasts comprised of gray to red porphyritic rocks of dacitic to andesitic composition (58.5 - 66.5 vol.% SiO_2) reach up to 10 mm. Subrounded to rounded pumice clasts range from creamy white to pale yellow in colour. They are relatively dense to finely vesicular and usually porphyritic, depending on degree of welding and contain predominantly augite and plagioclase as phenocrystals. Within the matrix, pumice clasts usually do not exceed diameters of 6 mm. Rare accessory clasts, red clay-siltstones and gray carbonate rocks, were derived from the subvolcanic basement and belong to the underlying Balsas Group and Cretaceous limestones.

The lava facies, represented by andesites and dacites are interpreted as viscous, slow moving blocky lava flows [57, 58] as they are associated with lava domes and coulées [59, 60].

4.1.2. Tuff samples

The massive pumice-rich tuffs exhibit of accessory and minor accidental lithic fragments (up to 10 cm in diameter) in a matrix of bubble wall shards and phenocrysts (feldspars, augite,

rare quartz). Accessory lithic clasts are comprised of gray to red porphyritic rocks of dacitic to andesitic composition (58.5 - 66.5 vol.% SiO_2) [61]. Pumice clasts range from creamy white to pale yellow in color. They are relatively dense to finely vesicular and usually porphyritic, containing predominantly augite and plagioclase as phenocrysts. Within the matrix, pumice clasts usually do not exceed diameters of 6 mm. However, in pumice concentration zones on top of single units, clasts can reach up to 10 cm in diameter. The colour of the tuff samples, varying from creamy beige to reddish purple, reflects the changes in the degree of welding and alteration. The welding range is subdivided into the four facies of welding [35]: 1) nonwelded, 2) incipiently welded, 3) partially welded, and 4) densely welded. The principal hydrothermal minerals in the samples include silica polymorphs, montmorillonite, and hematite. Most of the hydrothermal alteration in the welded tuff occurs as fracture and cavity fillings.

This lithofacies is interpreted as ash-flow deposit and is described by many authors as the most common ignimbrite lithofacies [62, 63, 64, 65].

4.1.3. Tuffaceous breccia samples

The tuffaceous breccia is composed of angular to subangular clasts in a pinkish red matrix of fine to medium sand. In outcrops, the clast size usually is in the range of pebbles and cobbles, not exceeding diameters of 20 cm; however, single outsized clasts of 2 m in diameter have been observed. The matrix of the deposits is commonly composed of lithic and pumice fragments, crystals and glass shards, showing significant alteration to clay minerals. The fragments do not show any alignment within the matrix.

The poor sorting and massive appearance are evidence for transport and deposition of this lithofacies by and from debris flows [66, 67, 68, 69, 70].

4.1.4. Siliciclastic rock samples

The sampled conglomerates and sandstones predominantly consist of lithic and pumice fragments, glass shards and crystals, indicating significant reworking of primary pyroclastic material and lava.

4.2. Permeability and porosity

Variations in permeability are correlated with lithology, alteration, and, in case of the tuff samples, with degree of welding. The highest permeabilities within the Tepoztlán Formation rocks can be found in the siliciclastic rock samples (mean $2.8 \cdot 10^{-14}$ m^2), followed by the tuffs (mean of $2.7 \cdot 10^{-14}$ m^2), tuffaceous breccias (mean $2.2 \cdot 10^{-14}$ m^2), and lavas exhibiting the lowest mean values of $9.7 \cdot 10^{-16}$ m^2 (Table 1). The permeabilities of the tuff samples can, furthermore, be distinguished according to their degree of welding (Table 2) into: 1) non-welded (mean $5.1 \cdot 10^{-15}$ m^2), 2) incipiently welded (mean $6.4 \cdot 10^{-14}$ m^2), 3) partially welded (mean $2.2 \cdot 10^{-14}$ m^2), and 4) densely welded (mean $3.8 \cdot 10^{-16}$ m^2).

Porosity values taken from Lenhardt and Götz [35] show that the lavas are characterized by the highest porosity values (mean of 30%) followed by tuffs, (mean 25.6%), conglomerates (mean 32.3%), sandstones (mean 18.9%) and the tuffaceous breccias showing the lowest porosities with mean values of 15.2%. The relatively high porosities of the lava samples can be explained by numerous vesicles and gas pockets in the lava. The tuff samples have a large range in measured porosity that corresponds to differences in welding and compaction after emplacement. The welding range can be subdivided into four distinct welding facies [35]: 1) incipiently welded (> 36%), 2) partially welded (36-30%), 3) moderately welded (30-2%), and 4) densely welded (< 2%). Generally, a steady decrease in porosity can be noticed from incipiently (mean of 37.7%) to densely welded tuffs with strongly reduced porosities (mean of 1.6%).

The permeability and porosity values from Tepoztlán are similar to those reported for other geothermal systems. Most volcanic-hosted geothermal systems have relatively low matrix

permeability, and thus fluid flow and bulk permeability are typically controlled by fractures. Bulk reservoir permeability values usually range between 1 and 100 mD ($9.9 \cdot 10^{-16}$ $m^2$to $9.9 \cdot 10^{-14}$ m^2) [71]. The Wairakei and Broadlands geothermal fields in New Zealand, for instance, have rhyolitic tuff reservoir rocks with reported permeabilities of $3.5 \cdot 10^{-14}$ m^2 to $4.0 \cdot 10^{-14}$ m^2 and $3.0 \cdot 10^{-14}$ m^2, respectively, and porosities of 20% [71, 72].

4.3. Thermal conductivity

Thermal conductivity data of the different rock types are plotted in Fig. 3. Ranges and mean values for individual rock types are given in Table 1, for the four facies types of tuffs in Table 2. The lava samples within the study area yield a mean conductivity of 1.5 W/(m·K), and a range from 1.0 to 1.9 W/(m·K).

Generally, the conductivity of the tuffs shows a range from 0.4 to 2.0 W/(m·K) (mean of 0.9 W/(m·K)). For non-welded tuffs the thermal conductivity ranges from 0.4 to 0.8 W/(m·K) (mean of 0.5 W/(m·K)). Incipiently welded tuffs have measured conductivities ranging from 0.4 to 0.8 W/(m·K) (mean of 0.6 W/(m·K)). Partially welded tuffs have conductivities ranging from 0.5 to 1.7 W/(m·K) (mean of 0.9 W/(m·K)). Densely welded tuffs have measured conductivities ranging from 1.5 to 2.0 W/(m·K) with a mean of 1.7 W/(m·K).

The thermal conductivity of the mass-flow deposits shows a range between 0.6 and 0.9 W/(m·K) (mean 0.8 W/(m·K)). Finally, fluvial deposits show thermal conductivities ranging between 0.4 and 0.9 W/(m·K) (mean 0.7 W/(m·K)).

5. Discussion

Despite the obvious advantages of the use of clean and safe geothermal energy sources, there are also some major disadvantages to it. Among others, the high installation costs are one major setback as power plants, electricity towers and stations need to be set up in order to transport the power from the geothermal plant to the consumer. This needs skilled staff, that

has to be recruited and then relocated to the place of interest, sometimes far away from major cities where the power is needed. The transport of the power from the plant to the consumer without too much loss is therefore one of the major challenges for the future use of geothermal energy. In addition, geothermal sites close to volcanic centres may contain poisonous and/or corrosive gases such as HCl and HF that can escape from the depth and be harmful to well casings or shallower aquifers that are used for drinking water extraction. In the Mexican Los Humeros geothermal reservoir, for instance, HCl steam is produced by the flow of fluids from a deep dry reservoir to a shallow water-saturated reservoir [74], resulting in corrosion and scaling due to fluid mixing and reacting with casing and rock [75]. The geothermal field of Cerro Prieto, in turn, is located far away from major cities where its power is needed. Both major disadvantages, i.e. the distance to the consumer and the corrosive gases, can be overcome by using the natural geothermal gradient of Mexico's deep sedimentary basins such as the Valley of Mexico with a depth of more than 4000 m. So far, the Valley of Mexico was not even taken into consideration for the use of deep geothermal energy. However, the results of the present study show the basin's favourable conditions and its similarities to other sedimentary basins whose geothermal potential is currently being assessed (e.g. the Pannonian Basins System of Rumania and Hungary) or already harvested (e.g the Molasse Basin in Germany, the Wei River Basin in China). The term "deep geothermal" is used for boreholes, which tap geothermal energy at depths exceeding 400 m, and at temperatures above 20°C [76]. Using deep geothermal energy either involves natural hot water resources (hydrothermal plants) or the heat stored in the rock (petrothermal plants). Both can be used to supply heat (at temperatures above ca. 60°C) and for power generation – usually at temperatures above ca. 100°C [76], with >150°C for dry steam power plants and >180°C for flash steam power plants [77, 78, 79]. Nevertheless, especially in low-to-medium temperature (~60-170°C), water-dominated geothermal fields, the binary-cycle method [80, 81, 82] has made considerable progress for electricity production [83, 84, 85, 86]. The deep

groundwater with a temperature of 163°C at a depth of ca. 2500 m as it was calculated by Fournier [50] and Edmunds et al. [25] for the Valley of Mexico would therefore be very much suitable for electricity production in a binary geothermal power plant.

According to the geothermal map of North America [87], the area of the Valley of Mexico shows an intermediate terrestrial heat flow of 80-84 mW/m^2. Compared to areas such as Cerro Prieto (~100 mW/m^2) [88] and Las Tres Vírgenes (117 mW/m^2) [89], located at thermal anomalies, this may not seem too impressive. The heat flow values of Los Azufres (84 mW/m^2) [90] and Los Humeros (85 mW/m^2) [90], however, show that the terrestrial heat flow values of the Valley of Mexico are still within a useable range. If compared to other international terrestrial heat flow and temperature data of sedimentary basins where deep geothermal energy is currently assessed or already harvested, one can, furthermore, see the potential of the Valley of Mexico. In Germany, for instance, areas such as the Molasse Basin in the South (geographically the area between the Danube and the Alps), the Upper Rhine Graben and the North German Basin are already used for geothermal energy. According to BINE [76], in the southern Molasse Basin, groundwater with temperatures of 70-140°C at 800-4500 m depth (heat flow of 80 mW/m^2 [91] and very similar to the conditions in the Valley of Mexico) is already used to produce electricity. The same applies for the Upper Rhine Graben were temperatures of 135-160°C are measured at depths of 2500-3300 m (heat flow of >100 mW/m^2) [91], and northern Germany with groundwater temperatures of 55-170°C at depths of 1300-3800 m.

The geothermal energy that is already harvested in China is mostly exploited (a lot more areas are currently under assessment) from sedimentary geothermal systems (e.g. North China and Wei River Basins) with low-medium temperature resources (groundwater temperatures of 40-120°C at 1500-4100 m and heat flow values of 55-80 mW/m^2) [92, 93, 94, 95]. This is because the population and economic activities are mainly distributed in the eastern part of China where low-medium resources are abundant, similar to the Valley of Mexico.

Finally, in Rumania and (western and southeastern) Hungary, where the geothermal potential is currently assessed [96], groundwater temperatures of 60-120°C at 800-3500 m [97] (heat flow 37-83 mW/m^2) [98], and 150-200°C at a depth of 3000-4000 m [99] (heat flow 90-100 mW/m^2) [100] are measured, respectively.

All these basins are dominated by clastic sedimentary and partly fractured and karstic limestone or dolomite successions with permeabilities and effective porosities of clastic and carbonate rocks similar to those of the Tepoztlán Formation. The here presented thermophysical rock properties of the volcano-sedimentary succession within the Valley of Mexico and its outcrop analogue Tepoztlán Formation show, that its tuffs and siliciclastic rocks qualify as target horizons for utilization of deep geothermal reservoirs. Both potential reservoir rock types are widespread in the volcano-sedimentary succession of the Valley of Mexico and are therefore very promising exploration targets with respect to hydrothermal power generation utilizing geothermal energy of deep sedimentary basins. Applying the thermofacies concept of [73], the low permeable tuffs (measured permeabilities at Cerro Prieto also only reach 10^{-14} m^2) [101] and siliciclastic rocks represent transitional (stimulated) systems, and depending on the degree of fracturing within the deeper part of the Valley of Mexico represent hydrothermal systems, respectively. Due to the high fracture porosity and the well developed fracture and cavity network in the Valley of Mexico [33], this area is well suited for hydrothermal systems.

Due to the limited access to existing borehole data (e.g. PEMEX), the here presented thermophysical rock properties of the different lithofacies types studied in outcrop sections add valuable information to the assessment of the geothermal potential of the Valley of Mexico. Thermophysical data from outcrop analogues serve to identify exploration target horizons and are important attributes for reservoir modelling.

Furthermore, the here presented poroperm data point to lithologies and areas of high potential for energy storage, i.e. compressed air energy storage and underground thermal energy storage, in the Valley of Mexico.

6. Conclusion

A first assessment of the geothermal potential of the Valley of Mexico is based on thermophysical data gained from outcrop analogues, covering all lithofacies types, and evaluation of groundwater temperature and heat flow values from literature. Comparison with data from other sedimentary basins where deep geothermal reservoirs are identified, shows the high potential of the Valley of Mexico for future geothermal reservoir utilization. The mainly low permeable lithotypes may be operated as stimulated systems, depending on the fracture porosity in the deeper subsurface. In some areas also auto-convective thermal water circulation might be expected and direct heat use without artificial stimulation becomes reasonable. The here presented data serve to identify exploration areas and are valuable attributes for reservoir modelling, contributing to (1) a reliable reservoir prognosis, (2) the decision of potential reservoir stimulation, and (3) the planning of long-term efficient reservoir utilization.

Acknowledgements

This study is part of a pilot project on reservoir characteristics of volcaniclastic rock series as outcrop analogues for geothermal reservoirs of world-wide importance. N.L. acknowledges the financial support of the National Research Foundation of South Africa (NRF) (grant no. 90800) and the University of Pretoria. A.E.G. acknowledges the support of the NRF (grant no. 85354) and Rhodes University (RC grant).

References

[1] Flores-Armenta M, Gutiérrez-Negrín LCA. Geothermal activity and development in Mexico. In: Short Course on Geothermal Drilling, Resource Development and Power Plants. Santa Tecla, El Salvador, 16-22 January 2011; 2011. Available at: http://www.os.is/gogn/unu-gtp-sc/UNU-GTP-SC-12-04.pdf; April 22, 2014.

[2] SENER (Secretaria de Energia) and GTZ (Deutsche Gesellschaft für Technische Zusammenarbeit). Renewable energies for sustainable development in Mexico. Available at: http://www.sener.gob.mx/res/PE_y_DT/pe/FolletoERenMex-SENER-GTZ_ISBN.pdf; April 22, 2014.

[3] World Energy Council. 2010 Survey of Energy Resources. Available at: http://www.worldenergy.org/documents/ser_2010_report_1.pdf; April 22, 2014.

[4] World Energy Council. Solar in Mexico. Available at: http://www.worldenergy.org/data/resources/country/mexico/solar; April 22, 2014.

[5] World Energy Council. Wind in Mexico. Available at: http://wec.bang-on.net/data/resources/country/mexico/wind; April 22, 2014.

[6] IEA (International Energy Agency) Wind. Annual report 2012. Available at: http://www.ieawind.org/annual_reports_PDF/2012/Mexico.pdf; April 22, 2014.

[7] Wood D, Lozano Medecigo S, Romero-Hernandez O, Romero-Hernandez S. Wind Energy Potential in Mexico's Northern Border States May 2012. Washington DC, USA: Woodrow Wilson International Center for Scholars; 2012. Available at:

http://www.wilsoncenter.org/sites/default/files/Border_Wind_Energy_Wood_0.pdf; April 22, 2014.

[8] Konrad J, Carriveau R, Davison M, Simpson F, Ting DS-K. Geological compressed air energy storage as an enabling technology for renewable energy in Ontario, Canada. Int J Environ Stud 2012; 69(2): 350-359.

[9] Kushnir R, Ullmann A, Dayan A. Thermodynamic and hydrodynamic response of compressed air energy storage reservoirs: A review. Rev Chem Eng 2012; 28(2-3): 123-148.

[10] McGrail BP, Cabe JE, Davidson CL, Knudsen FS, Bacon DH, Bearden MD, Chamness MA, Horner JA, Reidel SP, Schaef HT, Spane FA, Thorne PD. Techno-economic Performance Evaluation of Compressed Air Energy Storage in the Pacific Northwest. Washington State University, USA: Pacific North West Laboratory; 2013. Available at: http://caes.pnnl.gov/pdf/PNNL-22235.pdf; April 22, 2014.

[11] Sanner B, Karytsas C, Mendrinos D, Rybach L. Current status of ground source heat pumps and underground thermal energy storage in Europe. Geothermics 2003; 32(4): 579-588.

[12] Gao Q, Li M, Yu M, Spitler JD, Yan YY. Review of development from GSHP to UTES in China and other countries. Renew Sust Energ Rev 2009; 13(6-7): 1383-1394.

[13] Socaciu LG. Seasonal sensible thermal energy storage solutions. LEJPT 2011; 10(19): 49-68.

[14] Lu F, Du XJ, Zhou Y, Du YY. New progress of study in energy storage area of volcanic rocks. Adv Mater Res 2013; 616-618: 100-103.

[15] Boid N, Dronsfield S. Storing heat underground. Geodrilling International 2013; 3: 24-25.

[16] Wong B, Snijders A, McClung L. Recent inter-seasonal underground thermal energy storage applications in Canada. In: Proceedings of 2006 IEEE EIC Climate Change Technology Conference, EICCCC 2006; 2007: art. no. 4057362.

[17] GENI. Energy Overview of Mexico. Available at: http://www.geni.org/globalenergy/library/national_energy_grid/mexico/LatinAmericanPowerGuide.shtml; April 22, 2014.

[18] Geothermal Energy Association. 2013 Geothermal power: international market overview. Available at: http://geo-energy.org/events/2013%20International%20Report%20Final.pdf; April 22, 2014.

[19] World Energy Council. Geothermal in Mexico. Available at: http://www.worldenergy.org/data/resources/country/mexico/geothermal; April 22, 2014.

[20] Bertani R. Geothermal power generation in the world 2005–2010 update report. Geothermics 2012; 41: 1-29.

[21] Gutiérrez-Negrín LCA, Maya-González R, Quijano-León JL. Current Status of Geothermics in Mexico. In: Proceedings World Geothermal Congress 2010 Bali, Indonesia,

25-30 April 2010; 2010. Available at: http://geotermia.org.mx/geotermia/pdf/Mexico-2010.pdf; April 22, 2014.

[22] Gómez-Tuena A, Orozco-Esquivel MaT, Ferrari L. Igneous petrogenesis of the Trans-Mexican Volcanic Belt. In: Alaniz-Álvarez SA, Nieto-Samaniego, AF, editors. Geology of México, Geol Soc Am Spec Pap 2007; 422: 142-145.

[23] EIA (U.S. Energy Information Administration). Electric Power Industry – U.S. Electricity Imports from and Electricity Exports to Canada and Mexico, 2002-2012. Available at: http://www.eia.gov/electricity/annual/html/epa_02_13.html; April 22, 2014.

[24] Lund JW, Freeston DH, Boyd TL. Direct utilization of geothermal energy 2010 worldwide review. Geothermics 2011; 40: 159-180.

[25] Edmunds WM, Carrillo-Rivera JJ, Cardona A. Geochemical evolution of groundwater beneath Mexico City. J Hydrol 2002; 258: 1-24.

[26] Huizar-Alvarez R, Carrillo-Rivera JJ, Ángeles-Serrano G, Hergt T, Cardona A. Chemical response to groundwater extraction southeast of Mexico City. Hydrogeol J 2004; 12: 436-450.

[27] Peñuela-Arévalo LA, Carrillo-Rivera JJ. Discharge areas as a useful tool for understanding recharge areas, study case: Mexico Catchment. Environ Earth Sci 2013; 68: 999-1013.

[28] Birkle P, Torres Rodríguez V, González Partita E. Effects of evapotranspiration on the water balance of the Valley of Mexico. Geofís Int 1995; 35: 63-72.

[29] Birkle P, Torres Rodríguez V, González Partita E. The water balance for the Basin of the Valley of Mexico and implications for future water consumption. Hydrogeol J 1998; 6: 500-517.

[30] Ortega A, Cherry JA, Rudolph DL. Large-scale aquitard consolidation near Mexico City. Groundwater 1993; 31: 708-718.

[31] Ortega-Guerrero MA, Rudolph LD, Cherry JA. Analysis of long-term land subsidence near Mexico City: field investigations and predictive modeling. Water Resour Res 1999; 35: 3327-3341.

[32] Marsal RJ, Graue R. El subsuelo del lago de Texcoco. In: Nabor C, editor. El hundimiento de la Ciudad de México y Proyecto Texcoco, México, D.F.: Secretaría de Hacienda y Crédito Público; 1969, p. 167-202.

[33] Carrillo-Rivera JJ, Cardona A. Groundwater flow system response in thick aquifer units: theory and practice in Mexico. In: XXXIII-IAH Internacional Congress, Zacatecas, México. Asociación Internacional de Hidrogeólogos. Leiden, The Netherlands: Taylor & Francis Group 2008; 12: 25-46.

[34] Carrillo-Rivera JJ, Cardona A, Hergt T, Huizar AR, Kobr M. Marco geológico, hidrología subterráqnea, hidrogeoquímica, análisis geomorfológico y registros de temperatura en la subcuenca del río de las Avenidas. Final Report. Hidalgo, Mexico: CAASIM; 1999.

[35] Lenhardt N, Götz AE. Volcanic settings and their reservoir potential: an outcrop analogue study on the Miocene Tepoztlán Formation, Central Mexico. J Volcanol Geotherm Res 2011; 204: 66-75.

[36] Carrillo-Rivera JJ, Ángeles-Serrano G, Hergt T. Marco hidrogeológico conceptual a considerar en políticas de manejo de un área de descarga, caso: San Gregorio-Xochimilco. (Hydrogeological conceptual framework to be considered in management policy of a discharge area. Case: San Gregorio-Xochimilco). 28 Taller México-Cuba sobre las ciudades, el recurso agua, y el manejo de cuencas hidrológicas. La Habana, Cuba; 2003.

[37] Ferrari L, López Martínez M, Gonzalez Cervantes N, Jacobo Albarrán J, Hernandez Bernal M. Volcanic record and age of formation of the Mexico City Basin. 99th GSA Cordilleran Meeting 2003 Puerto Vallarta, Mexico, 1-3 April 2003; 2003.

[38] Lenhardt N, Böhnel H, Wemmer K, Torres-Alvarado IS, Hornung J, Hinderer M. Petrology, magnetostratigraphy and geochronology of the Miocene volcaniclastic Tepoztlán Formation: implications for the initiation of the Transmexican Volcanic Belt (Central Mexico). Bull Volcanol 2010; 72: 817-832.

[39] Lenhardt N, Hornung J, Hinderer M, Böhnel H, Torres-Alvarado IS, Trauth N. Build-up and depositional dynamics of an arc front volcaniclastic complex: The Miocene Tepoztlán Formation (Transmexican Volcanic Belt, Central Mexico). Sedimentology 2011; 58: 785-823.

[40] Lenhardt N, Böhnel H, Hinderer M, Hornung J. Paleocurrent direction measurements in a volcanic setting by means of anisotropy of magnetic susceptibility: A case study from the

Lower Miocene Tepoztlán Formation (Transmexican Volcanic Belt, Central Mexico). Sed Geol 2013; 290: 1-14.

[41] Lenhardt N, Herrmann M, Götz AE. Palynomorph preservation in volcaniclastic rocks of the Miocene Tepoztlán Formation (Central Mexico) and implications for paleoenvironmental reconstruction. Palaios 2013; 28(10): 710-723.

[42] Vázquez-Sánchez E, Jaimes-Palomera R. Geología de la Cuenca de México. Geofís Int 1989; 28: 133-190.

[43] Mooser F, Molina C. Estratigrafia y estructuras del valle de Mexico. Proceedings of Symposium: El subsuelo de la Ciudad de Mexico y su relacion con la ingeniera de cimentaciones. A cinco anos del sismo de 1985. Mexico DF: SMMS; 1993.

[44] De Cserna Z, De la Fuente-Duch M, Palacios-Nieto M, Triay L, Mitre-Salazar LM, Mota-Palomino R. Estructura geológica-gravimetria sismicidad y relaciones neotectónicas regionales de la Cuenca de México. Univ Nat Autón Méx Inst Geol Bull 1987; 104: 71.

[45] Durazo J, Farvolden RN. The groundwater regime of the Valley of Mexico from historic evidence and field observations. J Hydrol 1989; 112: 171-190.

[46] Cortez A, Farvolden RN. Isotope studies of precipitation and groundwater in the Sierra de las Cruces, Mexico. J Hydrol 1989; 107: 147-153.

[47] Cerca M, Carreon-Freyre DC, Gutiérrez R. Instability of the urbanized flank of El Peñón del Marques volcanic edifice and its relation to land subsidence in Mexico City. Land

subsidence, associated hazards and the role of natural resources development. In: Proceedings of EISOLS 2010 Querétaro, Mexico, 17-22 October 2010. IAHS Publ 2010; 339: 219-223.

[48] SHCP. El hundimiento de la ciudad de México. Proyecto Texcoco, Volumen Nabor Carillo. México: Secretaría de Hacienda y Credito Público; 1969: 187 p.

[49] Ziagos JP, Blackwell DD, Mooser F. Heat flow in southern Mexico and the thermal effects of subduction. J Geophys Res 1985; 90(B7): 5410-5420.

[50] Fournier RO. Application of water geochemistry to geothermal explorationnand reservoir engineering. In: Rybeck L, Muffler LJP, editors. Geothermal systems, principles and case histories. New York: Wiley; 1981, p. 109-143.

[51] Arce JL, Layer PW, Morales-Casique E, Benowitz JA, Rangel E, Escolero O. New constraints on the subsurface geology of the Mexico City Basin: The San Lorenzo Tezonco deep well, on the basis of 40Ar/39Ar geochronology and whole-rock chemistry. J Volcanol Geotherm Res 2013; 266: 34-49.

[52] Capra L, Macías JL. Pleistocene cohesive debris flows at Nevado de Toluca Volcano, central Mexico. J Volcanol Geotherm Res 2000; 102: 149-167.

[53] García-Palomo A, Macías JL, Arce JL, Capra L, Garduño VH, Espíndola JM. Geology of Nevado de Toluca Volcano and surrounding areas, central Mexico. Boulder, Colorado, Geol Soc Am Map and Chart Series MCH089 2002, pp. 1-26.

[54] García-Palomo A, Macías JL, Garduno VH. Miocene to recent structural evolution of the Nevado de Toluca volcano region, Central Mexico. Tectonophysics 2000; 318: 281-302.

[55] Mooser F, Montiel A, Zúniga Á. Nueva mapa geológica de las cuencas de México, Toluca y Puebla - Estratigrafía, tectónica regional y aspectos geotérmicos. México: Comision Federal de Electricidad; 1996.

[56] Popov YA, Pribnow DFC, Sass JH, Williams CF, Burkhardt H. Characterization of rock thermal conductivity by high-resolution optical scanning. Geothermics 1999; 28: 253-276.

[57] MacDonald GA. Volcanoes. Engelwood Cliffs, NJ: Prentice-Hall; 1972.

[58] Mueller W. Volcanism and related slope to shallow marine volcaniclastic sedimentation: an Archean example Chibougamau, Quebec, Canada. Precamb Res 1991; 49: 1-22.

[59] Williams H, McBirney AR. Volcanology. San Francisco: Freeman and Cooper; 1979.

[60] Orton GJ. Volcanic environments. In: Reading HG, editor. Sedimentary Environments: Processes, Facies and Stratigraphy, Oxford: Blackwell Science; 1996, p. 485-567.

[61] Lenhardt N. Volcaniclastic successions of the southern edge of the Transmexican Volcanic Belt: evidence for the Miocene plate reorganisation in Central America (Morelos, Mexico). Ph.D. Thesis. Darmstadt, Germany: Darmstadt University of Technology; 2009. Available at: http://tuprints.ulb.tu-darmstadt.de/1405/ (accessed in April 2014).

[62] Ross CS, Smith RL. Ash-flow tuffs. Their origin, Geological Relations and Identification. US Geol Survey Prof Pap 1961; 366: 81 pp.

[63] Sparks RSJ. Grain size variations in ignimbrites and implications for the transport of pyroclastic flows. Sedimentology 1976; 23: 147-188.

[64] Wilson CJN, Walker GPL. Ignimbrite depositional facies: the anatomy of a pyroclastic flow. J Geol Soc Lond 1982; 139: 581-592.

[65] Branney MJ, Kokelaar P. Pyroclastic density currents and the sedimentation of ignimbrites. Mem Geol Soc Lond 2002; 27: 143 pp.

[66] Hampton MA. Competence of fine-grained debris flows. J Sediment Petrol 1975; 45: 834-844.

[67] Johnson AM, Rodine JR. Debris Flow. In: Brunsden D, Prior DB, editors. Slope Instability, Chichester: Wiley; 1984, p. 257-361.

[68] Smith GA, Lowe DR. Lahars: volcano-hydrologic events and deposition in the debris flow – hyperconcentrated flow continuum. In: Fisher RV, Smith GA, editors. Sedimentation in Volcanic Settings, Soc Econ Paleontol Mineral, Spec Publ 1991; 45: 59-70.

[69] Coussot P, Meunier M. Recognition, classification and mechanical description of debris flows. Earth-Sci Rev 1996; 40: 209-227.

[70] Pierson TC, Daag AS, Reyes PJD, Regalado MTM, Solidum RU, Tubianosa BS. Flow and deposition of post-eruption hot lahars on the east side of Mount Pinatubo, July-October 1991. In: Newhall CG, Punongbayan RS, editors. Fire and Mud, Eruptions and Lahars of Mount Pinatubo, Philippines, Philippines Institute of Volcanology and Seismology: Univ Washington Press; 1996, p. 921-950.

[71] Bodvarsson GS, Witherspoon PA. Geothermal reservoir engineering - Part I. Geothermal Science and Technology 1989; 2(1): 1-69.

[72] Mikisek P, Bignall G, Sepulveda F, Sass I. Effect of hydrothermal alteration on rock properties in active geothermal setting. In: Abstracts of the Contributions of the EGU General Assembly, Vienna. Geophysical Research Abstracts 2012; 14: EGU2012-7212-1.

[73] Sass I, Götz AE. Characterization of geothermal reservoirs: a thermofacies concept. Terra Nova 2012; 24: 142-147.

[74] Tello Hinojosa E, Verma MP, Tovar Aguado R. Origin of acidity in the Los Humeros, Mexico, geothermal reservoir. In: Proceedings World Geothermal Congress 2000 Kyushu-Tohoku, Japan, 28 May – 10 June 2000; 2000: 2959-2967.

[75] Verma MP, Tello Hinojosa E, Arellano V, Nieva D. Acidic fluid in Los Humeros geothermal reservoir: a preliminary outlook. In: Proceedings of the Twenty-Third Workshop on Geothermal Reservoir Engineering, Stanford CA, USA, 26-28 January 1998; 1998: SGP-TR-158.

[76] BINE, 2011. Tracking deep geothermal energy - Leibniz Institute for Applied Geophysics offers Internet access to basic data for deep geothermal energy. Projectinfo 09/2011. Available at: http://www.bine.info/fileadmin/content/Publikationen/Englische_Infos/ProjektInfo_0911_engl_internetx.pdf; April 22, 2014.

[77] Fridleifsson IB, Bertani R, Huenges E, Lund JW, Ragnarsson A, Rybach L. The possible role and contribution of geothermal energy to the mitigation of climate change. In: Hohmeyer O, Trittin T, editors. Proceedings of the IPCC Scoping Meeting on Renewable Energy Sources, Lübeck, Germany, 20-25 January 2008; 2008: 59-80. Available at: http://www.os.is/gogn/Introductory_Lectures_2009/IPCC%20Geothermal%2011%20Feb%202008.pdf (accessed March 2014).

[78] DiPippo R. Chapter 7 - Dry-Steam Power Plants. In: DiPippo R, editor. Geothermal Power Plants. 3rd ed, Boston: Butterworth-Heinemann; 2012, p. 131-150.

[79] Zarrouk SJ, Moon H. Efficiency of geothermal power plants: A worldwide review. Geothermics 2014; 51: 142-153.

[80] DiPippo R. Ideal thermal efficiency for geothermal binary plants. Geothermics 2007; 36: 276-285.

[81] DiPippo R. Chapter 8 - Binary Cycle Power Plants. In: DiPippo R, editor. Geothermal Power Plants. 3rd ed, Boston: Butterworth-Heinemann; 2012, p. 151-182.

[82] Franco A, Villani M. Optimal design of binary cycle power plants for water-dominated, medium-temperature geothermal fields. Geothermics 2009; 38: 379-391.

[83] Dickson MH, Fanelli M. What is geothermal energy? Internal report, Istituto di Geoscienze e Georisorse, Pisa, Italy: CNR; 2004.

[84] Erkan K, Holdmann G, Benoit W, Blackwell D. Understanding the Chena Hot Springs, Alaska, geothermal system using temperature and pressure data from exploration boreholes. Geothermics 2008; 37: 565-585.

[85] Lashin A. A preliminary study on the potential of the geothermal resources around the Gulf of Suez, Egypt. Arab J Geosci 2013; 6: 2807-2828.

[86] Procesi M, Cantucci B, Buttinelli M, Armezzani G, Quattrocchi F, Boschi E. Strategic use of the underground in an energy mix plan: Synergies among CO_2, CH_4 geological storage and geothermal energy, Latium Region case study (Central Italy). Appl Energy 2013; 110: 104-131.

[87] Blackwell DD, Richards M 2004. Geothermal Map of North America. AAPG, 1 sheet, scale 1:6,500,000.

[88] Espinosa-Cardeña JM, Campos-Enriquez JO. Curie point depth from spectral analysis of aeromagnetic data from Cerro Prieto geothermal area, Baja California, México. J Volcanol Geotherm Res 2008; 176: 601-609.

[89] Prol-Ledesma RM. Terrestrial heat flow in Mexico. In: Cermák V, Rybach L. editors. Exploration of the Deep Continental Crust, Berlin: Springer-Verlag; 1991, p. 475-485.

[90] Polak BG, Kononov VI, Prasolov EM, Sharkov IV, Prol-Ledesma RM, Gonzalez A, Razo A, Molina-Berbeller R. First estimations of terrestrial heat flow in the TMVB and adjacent areas based on isotopic composition of natural helium. Geofís Int 1985; 24: 465-476.

[91] Vedova BD, Lucazeau F, Pasquale V, Pellis G, Verdoya M. Heat flow in the tectonic provinces of the European Geotraverse. Tectonophysics 1991; 244: 57-74.

[92] Chen W, Chen J, Yun Q, Xu S, Huang J, Yao Z 1977. Geological results report of petroleum general investigation of Fin-Wei Basin. The Third General Investigation Exploration Team, Xianyang, China (in Chinese), 358 pp.

[93] Kang F. Sustainable Development of Geothermal Resources in China. In: Proceedings of World Geothermal Congress 2010 Bali, Indonesia, 25-29 April 2010; 2010. Available at: http://www.geothermal-energy.org/pdf/IGAstandard/WGC/2010/0505.pdf (accessed in April 2014).

[94] Wang K. General Characteristics of Geothermal Areas in China. In: Proceedings of World Geothermal Congress 2010 Bali, Indonesia, 25-29 April 2010; 2010.

[95] Wang G, Li K, Wen D, Lin W, Lin L, Liu Z, Zhang W, Ma F, Wang W. Assessment of geothermal resources in China. In: Proceedings of the 38th workshop on geothermal reservoir engineering, Stanford CA, USA, 11-13 February 2013; 2013: SGP-TR-198. Available at:

http://www.geothermal-energy.org/pdf/IGAstandard/SGW/2013/Wang.pdf (accessed in April 2014).

[96] Götz AE, Török Á, Sass I. Geothermal reservoir characteristics of Meso- and Cenozoic sedimentary rocks of Budapest (Hungary). Z Dt Ges Geowiss 2014; [in press].

[97] Cohut I, Bendea C. Geothermal development opportunities in Central and Eastern Europe. GRC Transactions 1997; 21: 121-128.

[98] Veliciu S, Šafanda J. Ground temperature history in Romania inferred from borehole temperature data. Tectonophysics 1998; 291: 277-286.

[99] Dövényi P, Horváth F, Drahos D. Hungary. In: Hurter S, Haenel R, editors. Atlas of Geothermal Resources in Europe. Publ No EUR 17811 of the European Commission 2002; 36-38: 29-35.

[100] Szanyi J, Kovács B. Utilization of geothermal systems in South-East Hungary. Geothermics 2010; 39: 357-364.

[101] Menzies AJ, Granados EE, Gutierrez Puente H, Ortega Pierres L. Modeling discharge requirements for deep geotermal Wells at the Cerro Prieto geotermal field, Mexico. In: Proceedings of the 20th workshop on geothermal reservoir engineering, Stanford CA, USA, 24-26 January 1995; 1995: SGP-TIL-150. Available at: http://www.geothermex.com/files/Menzies_1995-2.pdf (accessed in April 2014).

Figure captions

Figure 1. Location map of the Basin of Mexico and areas south of the basin exposing the Tepoztlán Formation (shaded in grey) (modified after [25] and [35]).

Figure 2. Cross-section through the Valley of Mexico and location of the sampled sections (modified after [55] and [35]).

Figure 3. Thermophysical properties of the Tepoztlán Formation reservoir rocks and their thermofacies classification following the thermofacies concept by Sass and Götz [73], describing a geothermal system depending on heat transport (convective/conductive).

Tables

Table 1. Summary of permeability and thermal conductivity measurements.

Table 2. Summary of permeability and thermal conductivity measurements of the Tepoztlán tuffs.

Table 1. Summary of permeability and thermal conductivity measurements.

Lithology	**Number of measurements**	**Range of permeability (m^2)**	**Permeability mean (m^2)**	**Range of thermal conductivity [W/(m·K)]**	**Thermal conductivity mean [W/(m·K)]**
Lava	24	$3.6 \cdot 10^{-16}$ to $2.9 \cdot 10^{-15}$	$9.7 \cdot 10^{-16}$	1.0 to 1.9	1.5
Tuff	69	$1.4 \cdot 10^{-16}$ to $1.9 \cdot 10^{-13}$	$2.7 \cdot 10^{-14}$	0.4 to 2.0	0.9
Tuffaceous breccia	6	$2.0 \cdot 10^{-14}$ to $2.8 \cdot 10^{-14}$	$2.2 \cdot 10^{-14}$	0.6 to 0.9	0.8
Sandstones	26	$1.3 \cdot 10^{-14}$ to $1.6 \cdot 10^{-13}$	$2.8 \cdot 10^{-14}$	0.4 to 0.9	0.7

Table 2. Summary of permeability and thermal conductivity measurements of the Tepoztlán tuffs.

Lithology	**Degree of welding**	**Number of measurements**	**Range of permeability (m^2)**	**Permeability mean (m^2)**	**Range of thermal conductivity [W/(m·K)]**	**Thermal conductivity mean [W/(m·K)]**
Tuff	non-welded	6	$2.7 \cdot 10^{-15}$ to $7.2 \cdot 10^{-15}$	$5.1 \cdot 10^{-15}$	0.4 to 0.8	0.5
Tuff	incipiently welded	17	$3.4 \cdot 10^{-16}$ to $1.9 \cdot 10^{-13}$	$6.4 \cdot 10^{-14}$	0.4 to 0.8	0.6
Tuff	partially welded	33	$1.6 \cdot 10^{-16}$ to $1.0 \cdot 10^{-13}$	$2.2 \cdot 10^{-14}$	0.5 to 1.7	0.9
Tuff	densely welded	13	$1.4 \cdot 10^{-16}$ to $5.9 \cdot 10^{-16}$	$3.8 \cdot 10^{-16}$	1.5 to 2.0	1.7


Basin of Mexico
98°45'W
N
0 10 20 km
Sierra de Pachuca
Lake Texcoco
Atzcapotzaco
Mexico City
19°30'N
Sierra de las Cruces
Sierra de Rio Frio
Sra. Sta. Caterina
Coyoacan
Tlapan
Chalco
Sierra Chichinautzin
N
USA
Guatemala
Tepoztlán
Malinalco

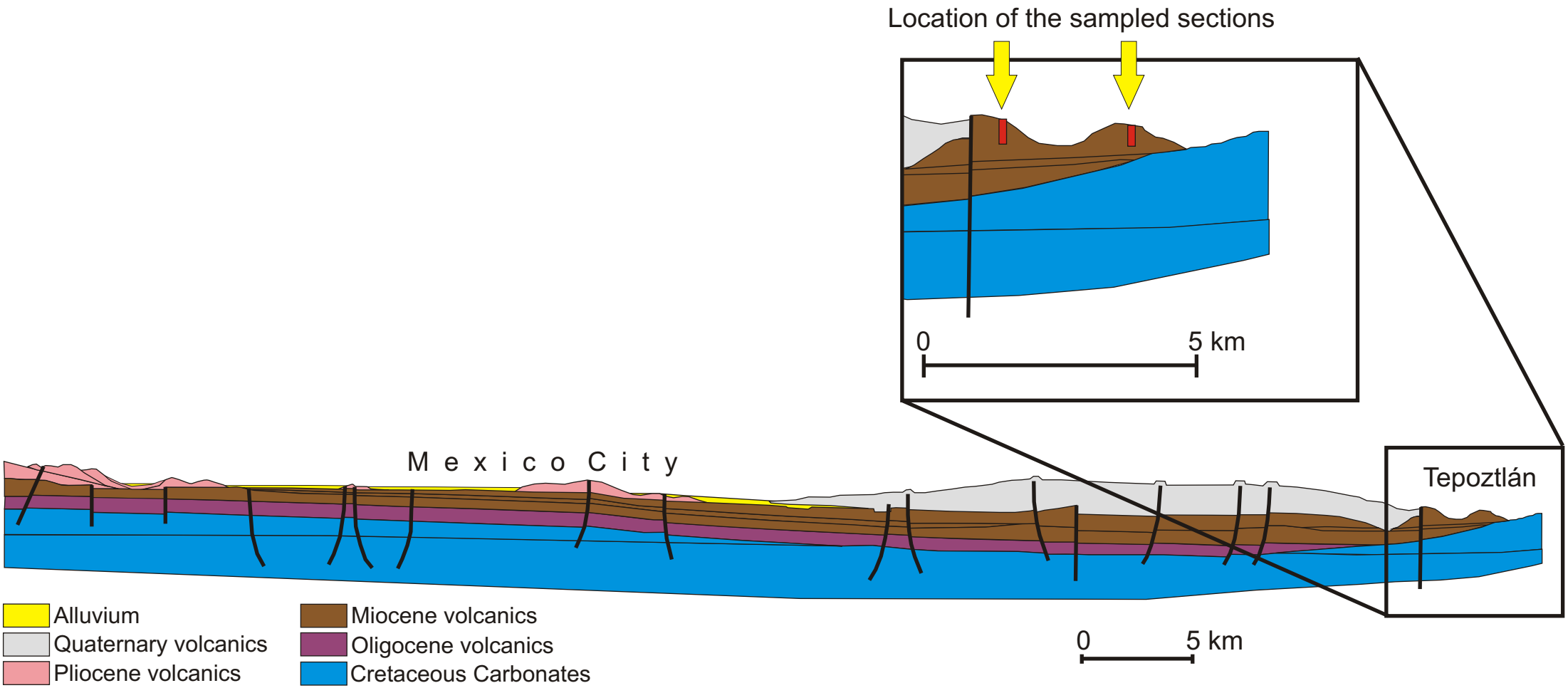
Location of the sampled sections
0
5 km
Tepoztlán
M e x i c o C i t y
0
5 km
Alluvium
Quaternary volcanics
Pliocene volcanics
Miocene volcanics
Oligocene volcanics
Cretaceous Carbonates

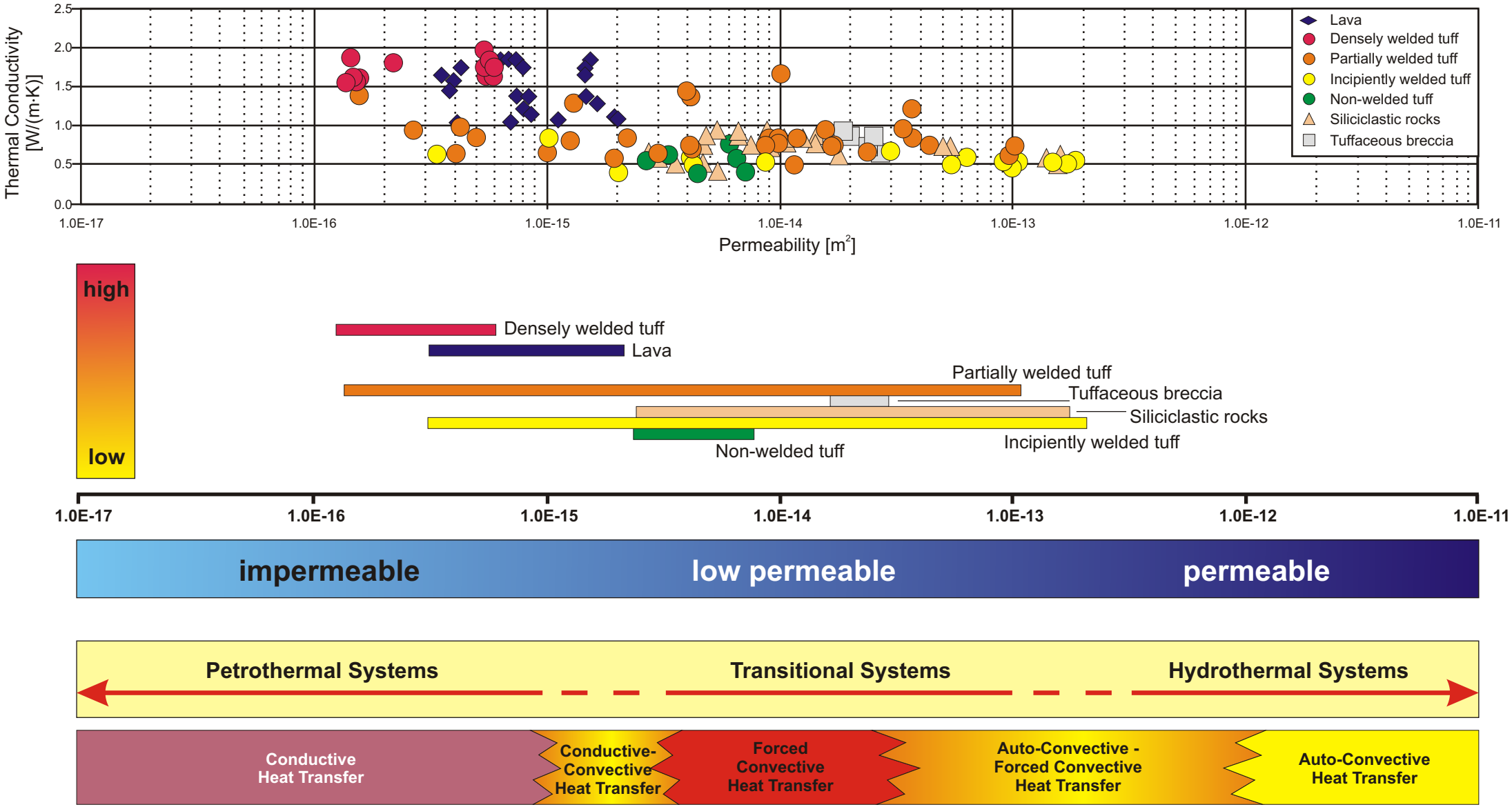
Thermal Conductivity [W/(m·K)]
2.5
2.0
1.5
1.0
0.5
0.0
1.0E-17
1.0E-16
1.0E-15
1.0E-14
1.0E-13
1.0E-12
1.0E-11
Permeability [m²]
Lava
Densely welded tuff
Partially welded tuff
Incipiently welded tuff
Non-welded tuff
Siliciclastic rocks
Tuffaceous breccia
high
low
Densely welded tuff
Lava
Partially welded tuff
Tuffaceous breccia
Siliciclastic rocks
Incipiently welded tuff
Non-welded tuff
1.0E-17
1.0E-16
1.0E-15
1.0E-14
1.0E-13
1.0E-12
1.0E-11
impermeable
low permeable
permeable
Petrothermal Systems
Transitional Systems
Hydrothermal Systems
Conductive Heat Transfer
Conductive-Convective Heat Transfer
Forced Convective Heat Transfer
Auto-Convective - Forced Convective Heat Transfer
Auto-Convective Heat Transfer